

# Coulomb proximity decay: A clock for measuring the particle emission time scale

S. Hudan, A.S. Botvina,\* R. Alfaro, L. Beaulieu, B. Davin, Y. Laroche, T. Lefort, V.E. Viola, H. Xu, R. Yanez, and R.T. de Souza  
*Department of Chemistry and Indiana University Cyclotron Facility  
Indiana University, Bloomington, IN 47405*

T.X. Liu, X.D. Liu, W.G. Lynch, R. Shomin, W.P. Tan, M.B. Tsang, A. Vander Molen, A. Wagner, and H.F. Xi  
*National Superconducting Cyclotron Laboratory and Department of Physics and Astronomy  
Michigan State University, East Lansing, MI 48824*

R.J. Charity and L.G. Sobotka  
*Department of Chemistry, Washington University, St. Louis, MO 63130*

(Dated: November 4, 2018)

## Abstract

A new method to examine the time scale of particle emission from hot nuclei is explored. Excited projectile-like and target-like fragments decay as they separate following a peripheral heavy-ion collision. Their mutual Coulomb influence results in an anisotropic angular distribution of emitted particles, providing a measure of the particle emission time scale. Predictions of a schematic evaporation model are presented and compared to experimental data.

PACS numbers: PACS number(s): 25.70.Mn

---

\*On leave from Institute for Nuclear Research, Moscow, Russia

While the decay of an isolated nucleus is well described by a statistical emission process[1], the decay in the presence of an external inhomogeneous field has only recently been considered[2]. Neutron stars with strong gravitational fields and heavy-ion collisions with strong Coulomb fields are environments in which such non-isolated decay may occur. In this Letter, we consider the Coulomb influence on the decay of a hot nucleus formed in a heavy-ion collision. For a nucleus at modest excitation ( $E^*/A \geq 2$  MeV), statistical model calculations predict decay on a relatively fast time scale,  $t \leq 100$  fm/c[3]. Directly measuring such short lifetimes is difficult[4] and is presently limited to a few approaches: two-fragment correlations[5, 6, 7] and near scission particle emission[8]. While two-particle correlations measure the time between successive emissions, and work at high excitation, near scission emission is restricted to relatively low excitation and the long time scale associated with fission. Other approaches such as the crystal blocking technique are sensitive to even longer time scales [9]. We describe a new approach to measuring the time scale of particle emission from hot nuclei, namely the angular anisotropy associated with Coulomb proximity decay.

For light fragments, Coulomb proximity decay has previously been used to explain the correlation between relative velocities of the decay products and their relative orientation[10] in terms of tidal forces[11]. For heavy projectile-like fragments, from in-plane angular distributions, the time between successive binary splittings[12, 13] has been deduced. In this analysis, we report for the first time on the influence of the external field on the probability for binary decay *and* the resulting angular distribution of emitted particles. Peripheral collision of two intermediate energy ( $E/A = 20$ -100 MeV) heavy-ions results in excited projectile-like and target-like fragments (PLF\* and TLF\* respectively) which de-excite as they separate with particle emission modified by their mutual Coulomb interaction. For a fixed separation distance between the PLF\* and TLF\*, and an asymmetric split of the PLF\*, emission of the smaller nucleus towards the TLF\* is favored due to the reduced Coulomb interaction between the three bodies[2, 14]. During the split, while the center-of-mass of the TLF\*-PLF\* system does not change, the center-of-mass of the PLF\* decay products can fluctuate. Although the influence of the external Coulomb field on the instantaneous breakup of a highly excited PLF\* has been reported[2, 14], we now examine the proximity influence on successive binary emissions and the resulting 'clock' of statistical emission.

To examine the main features of Coulomb proximity decay we have constructed a model in which the PLF\* with  $(Z,A)$ , characterized by a spin ( $J$ ) and excitation ( $E^*/A$ ), moves

away from the TLF\* with a velocity,  $V$ . For simplicity, the TLF\* is represented by a point source which does not undergo decay. Starting at an initial separation distance, the de-excitation of the PLF\* *via* sequential binary decays of light particles ( $n, Z \leq 2$ ) and heavy clusters (up to  $^{18}\text{O}$ ) is calculated using a Weisskopf approach[15]. In this model[16], the decay width for the emission of a particle  $j$  in the excited state  $i$  from a nucleus ( $Z, A$ ) is given by:

$$\Gamma_j^i = \int_0^{E_{AZ}^* - B_j - \epsilon_j^{(i)}} \frac{\mu_j g_j^{(i)}}{\pi^2 \hbar^2} \sigma_j(E) \frac{\rho_f(E_{CN}^* - B_j - E)}{\rho_{CN}(E_{CN}^*)} E dE \quad (1)$$

Here  $\epsilon_j^{(i)}$  ( $i = 0, 1, \dots, n$ ) is taken for the ground and all particle-stable excited states of the fragment  $j$ , and  $g_j^{(i)} = (2s_j^{(i)} + 1)$  is the spin degeneracy factor of the  $i$ -th excited state,  $\mu_j$  and  $B_j$  are corresponding reduced mass and separation energy,  $E_{CN}^*$  is the excitation energy of the initial compound nucleus (PLF\*), and  $E$  is the kinetic energy of an emitted particle in the center-of-mass of the emitting system. The level densities of the initial compound ( $A, Z$ ) and final ( $A_f, Z_f$ ) residual nuclei,  $\rho_{CN}$  and  $\rho_f$  are calculated using the Fermi-gas formula  $\rho(E) \propto \exp(2\sqrt{aE})$  with the level density parameter  $a \approx 0.125A\text{MeV}^{-1}$ . In the present work we have parametrized the cross-section as  $\sigma_j(E) = \pi R_{fj}^2 (1 - U_c/E)$ , where  $U_c$  is the Coulomb barrier for fragment emission and  $R_{fj} = R_f + R_j$ ,  $R_f = r_n A_f^{1/3}$ ,  $R_j = r_n A_j^{1/3}$ , with  $r_n = 1.5\text{fm}$ .

We modified this model by taking into account the influence of the external Coulomb field on the decay width. The daughter residue and emitted fragment are assumed to be touching spheres and are placed within a sphere of radius  $R_j + R_f$  with center located at the center-of-mass of the decaying parent (PLF\*) nucleus. The decay configuration within the sphere is impacted by the change in the Coulomb energy of the three-body system:

$$U_c = \frac{Z_f * Z_j}{R_{fj}} + \frac{Z_{TLF*} Z_j}{R_{TLF*j}} + \frac{Z_{TLF*} Z_f}{R_{TLF*f}} - \frac{Z_{TLF*} Z}{R_{TLF*CN}} \quad (2)$$

where  $Z_{TLF*}$  is the charge of the TLF\*, and  $R_{TLF*j}$ ,  $R_{TLF*f}$ ,  $R_{TLF*CN}$  are distances from the TLF\* to the emitted particle, residual nucleus and compound nucleus, respectively. The probability of fragment emission can be found by averaging eq. (1) over all coordinates of fragments. Since the Coulomb barrier is lower when the smaller fragment is emitted in the direction of the TLF\*, the resulting fragment emission is anisotropic in the PLF\* frame. The angular momentum of the PLF\* was included using a standard approach [14, 17].

The full width for evaporation is determined by summing up all emission channels:  $\Gamma = \sum \Gamma_j^i$ . The mean time for an emission step is given by  $\tau = \hbar/\Gamma$ . The PLF\* is assumed to

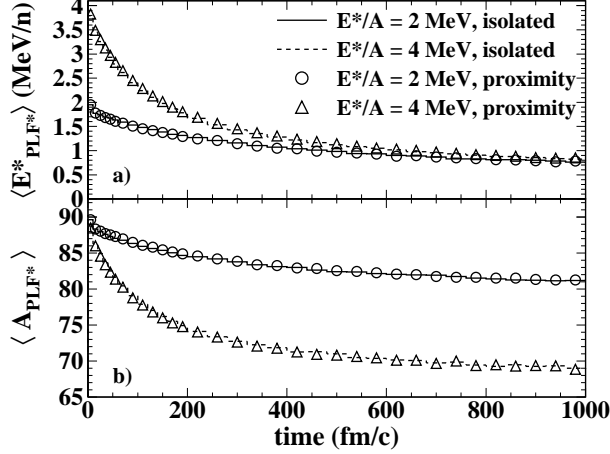


FIG. 1: Average excitation energy and mass number as a function of time for a nucleus decaying in an external field and an isolated nucleus.

have a lifetime,  $t$ , with a distribution  $\exp(-t/\tau)$ . Until the decay occurs, the PLF\*, TLF\*, and all charged particles propagate along Coulomb trajectories. Successive binary emissions, conserving energy and momentum, are calculated until the excitation energy is below the particle emission threshold.

For the results presented we assumed the PLF\* had  $Z=38$ ,  $A=90$  and was located at an initial distance of 30 fm from the TLF\* with spin  $J=10\hbar$  or  $J=40\hbar$ . This distance is compatible with an equilibration time of  $\approx 100$  fm/c following the collision in agreement with dynamical simulations[18]. The TLF\* was assumed to be a point source with  $Z=42$ ,  $A=114$ ,  $V=0.2728c$  relative to the PLF\* and interacted *via* the Coulomb interaction.

Displayed in Fig. 1 is the influence of the Coulomb proximity effect on the de-excitation of the PLF\* with  $J=10\hbar$ . The decay of an isolated PLF\*, not subject to the Coulomb proximity effect, is presented as a reference. The essentially identical behavior in both  $\langle E^*_{PLF^*} \rangle$  and  $\langle A_{PLF^*} \rangle$  as a function of time for both the isolated and proximity cases, indicates that for these initial conditions, the average rate of particle emission is comparable. For smaller initial PLF\*-TLF\* distances or larger TLF\* atomic number, however, the proximity influence can alter the particle emission rate as compared to the isolated case. The rapid de-excitation of the PLF\* is clearly evident for  $t \leq 250$  fm/c, corresponding to a PLF\*-TLF\* distance of  $\approx 70$ fm. Associated with the rapid decrease in excitation of the PLF\* is the corresponding decrease in the mass of the PLF\*, (Fig. 1b). For an initial excitation of  $E^*/A=4$  MeV, by  $t=250$  fm/c approximately 25% of the mass of the PLF\* has been emitted.

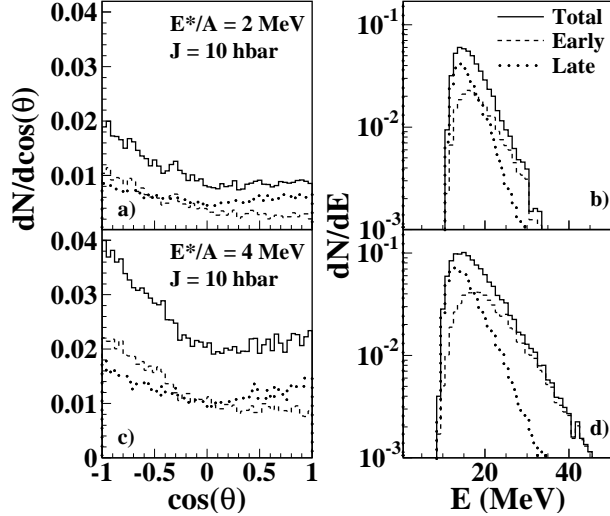


FIG. 2: Angular distributions and kinetic energy spectra of  $\alpha$  particles in the PLF\* frame selected on emission time.

Although the average excitation of the PLF\* at a given time, under these assumptions, is not appreciably affected by the Coulomb proximity, the angular distribution of emitted particles is impacted by the Coulomb field of the target, as shown in Fig. 2 for  $\alpha$  particles ( $E^*/A = 2$  and  $4$  MeV and  $J = 10\hbar$ ). For all cases, the angular distribution is peaked near  $\cos(\theta)=-1$ , corresponding to emission in the direction of the TLF\*. For the conditions calculated, emission towards the TLF\*, i.e.  $\cos(\theta)\approx-1.0$ , is enhanced in yield by a factor of 2 relative to  $\cos(\theta)\approx 0$ . To understand better the behavior of proximity emission we have selected on decays that occur at a distance  $\leq 70$  fm (i.e.  $\approx 250$  fm/c) and refer to these decays as early decays. Decays which occur at larger distances experience a negligible influence of the TLF\* Coulomb field and are referred to as late decays. While the late decays (dotted line) exhibit a symmetric and relatively isotropic distribution, the pronounced peak in the total angular distribution is associated with the early decays (dashed line) which are focused towards the TLF\* by the proximity Coulomb effect. The magnitude of the asymmetry for these early decays, can be assessed, to first order, by comparing the yield at  $\cos(\theta)=-1$  to  $\cos(\theta)=+1$ . At  $E^*/A=2$  MeV an asymmetry of  $\approx 4$  is observed.

The impact of the Coulomb proximity effect on the kinetic energy spectra of emitted particles is also shown in Fig. 2. In this figure, it is evident that, as expected[19], the tail of the  $\alpha$  particle kinetic energy distribution is preferentially populated by early emissions (dashed line). From the angular distributions presented in Fig. 2 it is clear that these

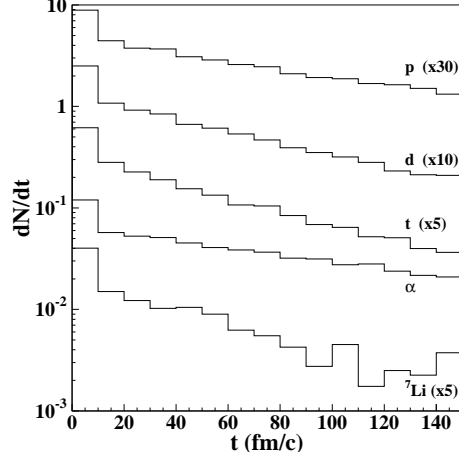


FIG. 3: Emission time distributions of emitted particles from the PLF\*.

emissions occur in the proximity of the TLF\*. Comparison of Fig. 2b and 2d shows that with increasing excitation, late emission (dotted line) provides an increasing contribution to the region of the Coulomb peak. For  $\alpha$  with  $E \leq 25$  MeV, the magnitude of the increase for the late emission is  $\approx 6\%$ . This result is understandable as with increasing excitation, an increasing amount of excitation energy remains at a PLF\*-TLF\* distance of 70 fm where the proximity effect is significantly reduced. The energy-angle correlations introduced by the Coulomb proximity effect present interesting opportunities in studying the de-excitation cascade of a hot nucleus. The angular asymmetry of  $\alpha$  particles resulting from proximity emission is related to the time spent by the PLF\* in the vicinity of the TLF\* and thus forms a 'clock' of the statistical emission time.

Another interesting aspect of the Coulomb proximity effect is that different emitted particles are sensitive to different portions of the de-excitation cascade. Depicted in Fig. 3 is the dependence of emission probability on time for p, d, t,  $\alpha$  and  ${}^7\text{Li}$  for  $E^* = 4$  MeV and  $J = 10\hbar$ . While the emission time distributions exhibited of  $\alpha$  particles, for example is relatively flat decreasing by only a factor of 3 over the time interval displayed, other particles e.g. t,  ${}^7\text{Li}$  exhibit steeper distributions. In the case of both t and  ${}^7\text{Li}$ , a decrease of more than one order of magnitude is observed. This behavior can be understood in terms of the Coulomb barrier and binding energy relative to the available excitation of the PLF\*. Particles such as  ${}^7\text{Li}$  therefore sample the earliest portion of the de-excitation cascade and thus exhibit an enhanced sensitivity to proximity emission. Comparison of the angular asymmetry of particles with different sensitivities can therefore provide multiple 'clocks' which probe the

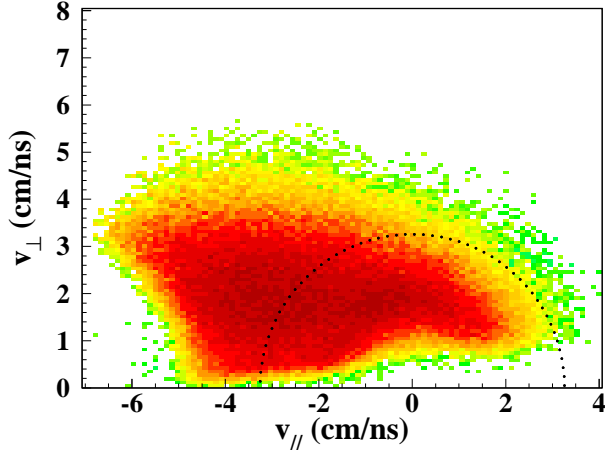


FIG. 4: Invariant cross-section map of  $\alpha$  particles in the PLF\* frame for the reaction  $^{114}\text{Cd} + ^{92}\text{Mo}$  at  $E/A = 50$  MeV.

statistical decay of a hot nucleus. Naturally, the Coulomb field of a particle emitted early also influences subsequent emissions. Consequently, this work represents the first step towards a theory of *interacting sequential decays*. As such it represents a significant departure from Bohr's independence hypothesis that is traditionally invoked.

In order to examine whether the asymmetries predicted by this schematic model are manifested in experimental data with comparable magnitude, we have compared the model predictions to data from the reaction  $^{114}\text{Cd} + ^{92}\text{Mo}$  at  $E/A=50$  MeV. In this experiment, detection of a PLF ( $15 \leq Z \leq 46$ ) at very forward angles ( $2.1^\circ \leq \theta_{lab} \leq 4.2^\circ$ ) together with measurement of the associated charged particles emitted at larger angles ( $7^\circ \leq \theta_{lab} \leq 58^\circ$ ) allow us to focus on particles emitted from the PLF\*[20]. The invariant cross-section map shown in Fig. 4, exhibits an essentially circular ridge of yield centered on the PLF\* velocity. This ridge has a radius corresponding to the Coulomb repulsion between the emitted  $\alpha$  and PLF\* residue suggesting that  $\alpha$  particles along this ridge are associated with emission from the PLF\*. Selecting  $\alpha$  particles on the ridge does not ensure statistical emission as dynamical processes may also contribute at the most backward angles[21]. Also evident in Fig. 4 is a peak at  $V_{||}=-4$  cm/ns and  $V_{\perp}=2$  cm/ns, attributable to mid-velocity emission[22, 23] that represents a background for the statistical component considered.

In Fig. 5a the angular distribution of  $\alpha$  particles with  $E_{\alpha} \leq 22$  MeV, i.e. along the ridge in Fig. 4, is displayed normalized to the yield at  $\theta=90^\circ$ . The data are backward peaked with an enhancement of a factor of  $\approx 2$ . The observed  $\alpha$  particle yield at forward angles,

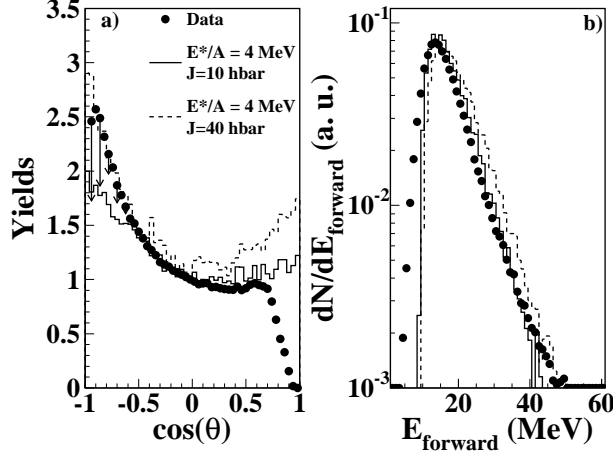


FIG. 5: Panel a: Comparison of angular distribution of  $\alpha$  particles from the reaction  $^{114}\text{Cd} + ^{92}\text{Mo}$  at  $E/A = 50$  MeV with  $E_\alpha \leq 22$  MeV in the PLF\* frame with results of the proximity decay model. Panel b: Kinetic energy spectra in the PLF\* frame of  $\alpha$  particles emitted forward of the PLF\*.

$\cos(\theta) \geq 0.65$ , and very backward angles,  $\cos(\theta) \leq -0.9$ , is suppressed due to the finite acceptance of the experimental setup. We have corrected for the mid-velocity emission contribution to the yield with  $E_\alpha \leq 22$  MeV by examining the kinetic energy distributions in the PLF\* frame selected on emission angle, as indicated by the representative arrows in Fig. 5. For  $\cos(\theta) \geq -0.7$  this contribution is negligible while for more backward angles a correction of upto 25% is observed. The excitation deduced by calorimetry, using forward emission and assuming isotropy, for the data shown in Fig 4 and 5 is  $\approx 2.3$  MeV/A[20]. The measured angular distribution is reasonably described by the model presented with  $E^*/A = 4$  MeV. The discrepancy between the experimentally deduced excitation and the initial excitation used in the model can be understood by the rapid cooling evident in Fig. 1. Inclusion of angular momentum at this excitation results in a more peaked angular distribution for  $\cos(\theta) \leq -0.7$ .

The kinetic energy spectrum of  $\alpha$  particles emitted in the forward direction is shown in Fig 5b. The experimental distribution is remarkably well described by the model, despite its simplicity. Increased angular momentum acts to broaden the peak of the distribution, as well as slightly extend the high energy tail of the distribution. While the exponential slope of the kinetic energy spectrum is somewhat better described by the  $10\hbar$  case, the width of the Coulomb peak is better described by the  $40\hbar$  case, perhaps suggesting that the experimental data is intermediate between these two cases, in agreement with the angular distributions



shown in Fig. 5a.

In summary, we have explored how Coulomb proximity decay can impact the statistical binary decay of a hot nucleus. As PLF\* and TLF\* separate following a peripheral heavy-ion collision, while the emission rate of particles from the PLF\* may be essentially unaffected, the angular distribution of emitted particles shows a pronounced effect. Emission of particles as the PLF\* and TLF\* separate occurs preferentially in the direction of the TLF\* resulting in an asymmetric angular distribution that reflects the amount of emission occurring in the vicinity of the TLF\*. This angular asymmetry for different emitted particles together with their associated kinetic energy spectra provides a clock of the emission timescale. Experimental data exhibit an asymmetry of comparable magnitude suggesting the applicability of this technique. Both the sensitivity of this clock and the deconvolution of dynamically emitted mid-rapidity particles can be assessed by modifying the magnitude of the external field by changing the target, modifying the velocity with which the PLF\* and TLF\* separate by changing the incident energy, or altering the excitation of the PLF\* by selecting different velocity dissipation[20].

### Acknowledgments

We would like to acknowledge the valuable assistance of the staff at MSU-NSCL for providing the high quality beams which made this experiment possible. This work was supported by the U.S. Department of Energy under DE-FG02-92ER40714 (IU), DE-FG02-87ER-40316 (WU) and the National Science Foundation under Grant No. PHY-95-28844 (MSU).

- 
- [1] T. Ericson, *Adv. in Phys.* **9**, 425 (1960).
  - [2] A. S. Botvina et al., *Phys. Rev. C* **59**, 3444 (1999).
  - [3] R. J. Charity, *Phys. Rev. C* **61**, 054614 (2000).
  - [4] D. Hilscher and H. Rossner, *Ann. Phys. (Paris)* **17**, 471 (1992).
  - [5] R. Trockel et al., *Phys. Rev. Lett.* **59**, 2844 (1987).
  - [6] E. Cornell et al., *Phys. Rev. Lett.* **75**, 1475 (1995).
  - [7] L. Beaulieu et al., *Phys. Rev. Lett.* **84**, 5971 (2001).

- [8] D. J.Hinde et al., Phys. Rev. C **45**, 1229 (1992).
- [9] F. Goldenbaum et al., Phys. Rev. Lett. **82**, 5012 (1999).
- [10] R. Charity et al., Phys. Rev. C. **63**, 024611 (2001).
- [11] R. Charity et al., Phys. Rev. C. **46**, 1951 (1992).
- [12] G. Casini et al., Phys. Rev. Lett **71**, 2567 (1993).
- [13] D. Durand et al., Phys. Lett. B **345**, 397 (1995).
- [14] A. Botvina et al., Phys. Rev. C **63**, 061601R (2001).
- [15] V. Weisskopf, Phys. Rev. **52**, 295 (1937).
- [16] A. Botvina et al., Nucl. Phys. A **475**, 663 (1987).
- [17] R. J. Charity et al., Nucl. Phys. A **483**, 371 (1988).
- [18] J. P. Bondorf et al., Phys. Rep. **257**, 133 (1995).
- [19] J. R. Huizenga et al., Phys. Rev. C **40**, 668 (1989).
- [20] R. Yanez et al., Phys. Rev. C **68**, 011602(R) (2003).
- [21] F. Bocage et al., Nucl. Phys. A. **676**, 391 (2000).
- [22] E. Plagnol et al., Phys. Rev. C **61**, 014606 (2000).
- [23] L. Gingras et al., Phys. Rev. C **65**, 061604(R) (2002).